ZIBELINE INTERNATIONAL™ PUBLISHING

ISSN: 2773-6202 (Online)
CODEN: JTIOCC

Journal of Technology and Innovation (JTIN)

DOI: http://doi.org/10.26480/jtin.01.2026.30.40

CrossMark

REVIEW ARTICLE

MICROSTRUCTURES AND ITS INFLUENCE ON THE DURABILITY OF CONCRETE : REVIEW

Kapilraj Natkunarajah and Masilamani Koneswaran*

Department of Chemistry, Faculty of Science, Eastern University Sri Lanka, Vantharumoolai, Chenkalady 30350, Sri Lanka.
****Corresponding Author Email: koneswaran@esn.ac.lk***

ARTICLE DETAILS

Article History:

Received 23 November 2025
Revised 15 December 2025
Accepted 21 January 2026
Available online 04 February 2026

ABSTRACT

The microstructure has an extreme impact on the durability of concrete. Many researchers focus on this area to understand the impact of microstructure on concrete durability. This review article discusses the microstructure present in the concrete such as porosity, permeability, and other factors that affect the durability of concrete. In addition, methods used in the durability test such as Mercury intrusion porosimetry, Nitrogen adsorption method, X-ray micro tomography, Sulphate attack, Half-Cell Potentials, and Rapid chloride permeability are also described. The overall analysis in this field shows that porosity and permeability are the main factors influencing the durability of cementitious materials. However, with enough hydration, porosity can be minimized to a certain extent. The permeability of cementitious material largely depends on several factors including sample preparation, curing conditions, type of media, and age of the sample. Water continuity, sulfate chloride attack, carbonation, and the alkali-aggregate reaction are extrinsic factors that affect concrete's durability. This review also discusses emerging research areas such as admixtures and sensors that are involved in health monitoring of concrete.

KEYWORDS

Alkali aggregate reaction, Chloride attack, Durability, Permeability, Porosity, Steel corrosion, Sulphate attack

1. INTRODUCTION

Over the decades, concrete has been a most used material. Every year, massive amounts of lime stones are utilized in the manufacturing of Portland cement. A large amount of CO_2 is emitted during the calcination process. As a result, Portland cement production has a considerable impact on global warming and the environment. During the production of one ton of Portland cement, approximately one ton of CO_2 is released to the environment (Malhotra and Mehta, 2002). A longer service life for a concrete construction minimizes both the financial loss and the demand for Portland cement. In addition, a concrete construction takes time and lots of money therefore, durability of such structure is crucially important.

Characteristics of hardened concrete can be speculated by measuring the hydration products at a different time which develops during hydration reaction. The overall strength and tightness of concrete are caused by mineral and chemical composition as well as the strength of the crystalline lattice of hydration products (Arandigoyen and Alvarez, 2007). Calcium-silicate-hydrate gel or C-S-H gel or tobermorite gel is the main product that causes the strength of concrete. The hardening mechanisms of cementitious materials rest on the hardness of tobermorite gel integrated with the addition of water and crystallization of calcium aluminium sulphate (ettringite) and calcium hydroxide (portlandite) intergrowths forming and filling pores in hardening cement paste (Franus et al., 2015).

Apart from the strengthening factors, concrete is a heterogonous and multiple-phase material. That consists of solid phases and pore phases. The solid phase contains coarse-aggregates, fine-aggregates, calcium hydroxide, and tobermorite, whereas the pore phases contain air voids, capillary pores, and gel pores. The microstructure of the surface zone of concrete structures governs the structure's durability. The number and location of pores in the surface zone, as well as their connectivity, have a significant impact on the concrete's long-term durability. The harmful substances that deteriorate concrete structures like chloride ions, penetrate through the interconnected capillary pores of the concrete matrix and reach the reinforced steel bar. These substances induce the corrosion of the concrete reinforced steel bar by reducing the pH of concrete pore solution (Ye and Van Breugel, 2009). The problem caused by the capillary pores in the concrete can be characterized by the degree of connectivity (Ye and Van Breugel, 2009). It is accepted that the connectivity of the solid phase in cementitious materials is the foundation for the development of the mechanical properties. Furthermore, the de-percolation of the liquid phase is crucial for the transport properties (Ye, 2005).

Concrete materials require reinforcement to improve tensile and flexural strength (Wang et al., 2018). However, formation of iron oxide due to the corrosion of reinforced-steel bar, expands its volume and makes the cracks (Ma, et al., 2017). Initially micro sized cracks are formed, and it facilitate transportation of ions, further it expands more. The durability of concrete is neither related to corrosion or concrete microstructure; it is affected by several factors such as carbonation, chloride migration, freezing-thaw weathering, sulphate attack, alkali leaching, alkali-aggregate reaction, etc. depending on the environment. Not only environmental impact, improper materials, fake designs, poor data collection, improper quality control, incomplete curing, etc. can also reduce the service life of the structures and lead to an economical loss (Ye and Van Breugel, 2009). The environmental and economic impact related to the durability problem of concrete material leads to extensive research for over two decades. Many test

Quick Response Code	Access this article online	
	Website: www.jtin.com.my	**DOI:** 10.26480/jtin.01.2026.30.40

methods, techniques, rules, and quality standards have been developed to make quality and durable construction material. Most researchers now focus on the micro or nanostructure and imbibition nature of concrete porous structure (Basheer, et al., 2001).

As mentioned above deteriorative substances travel through the interconnected pore, which reduces the pH of concrete pore solution and initiate the corrosion. This is the main process takes places concerning the durability of concrete. Reduce the porous nature of concrete and maintain a high pH value in the pore solution will increase concrete durability. Moreover, the addition of Nano-silica can be act as fillers and help to develop C-S-H gel into micro pores by the pozzolanic reaction. The improvement in the durability by the addition of Nano-silica has been proven experimentally by many researchers (Nandhini and Ponmalar, 2021). Indeed, the silica reacts with alkali present in the concrete matrix and produce the alkali silica products (ASR), later this product is converted into C-S-H (Shi and Lothenbach, 2019). However, this reaction can reduce the concrete's pH level.

Addition of pozzolanic materials can interfere with the hydration reaction of cement. Gypsum presents in the cement decrease the formation rate of C_3A, but addition of pozzolans oppose this reaction, and also it accelerates the hydration of C_3S (McCarthy and Dyer, 2019). In addition, there are several pozzolans have been tested by many researchers to improve the concrete properties concerning the durability (McCarthy and Dyer, 2019). The durability performance of Ultra High-Performance concrete containing meta kaolin show similar effect to silica fume (Tafraoui, et al., 2016). Addition of fly-ash is another way to improve the concrete durability. Fly ashes are finely separated particles formed when pulverized coal is burned to generate energy at power plants. Chemically, fly ash can be classified based on the coal type used and the primary oxides found. According to ASTM C618, Class F fly ash (siliceous) contains the sum of SiO_2, Al_2O_3 and Fe_2O_3 more than 70%. Class C (calcareous) fly ash contains more than 50% of above oxides, and class C fly ash generally has a higher total calcium level than Class F (McCarthy, et al., 2013). The durability property of concrete contain fly ash significantly increases and it exhibit excellent chloride resistance capacity (Dhandapani and Santhanam, 2019). However, the recent experimental results reveal that, partial replacement of cement by calcined clay (Calcined clay 31% + Limestone 15%) exhibited better durability property than of fly ash (30%) (Dhandapani and Santhanam, 2019). Disconnection of interconnected porous network was obtained earlier in the addition of calcined clay formula than the addition of fly ash (Dhandapani and Santhanam, 2019).

The proper use of instruments is critical to the long-term durability of concrete. The concrete structure in a service cannot be broken to check the quality parameters. In recent decades, several research studies have focused on developing non-destructive techniques to monitor concrete health. Optical pH sensors, Fluorescence based pH sensors, piezo-electric stress sensors, wireless electronic devices, chemical sensors are still being developed (Fan and Bao, 2020; Shamsipur et al., 2019; Das and Saha, 2018; Quinn, et al., 2012; Mamun, 2019). Early detection of faults/threatening factors allows for faster repair, extending the service life. However, the chemical and physical properties of concrete can be studied using a variety of analytical tools in the laboratory.

This review summarises most important factors that affect the concrete durability, factors consider during the sample preparation, mathematical parameters involved in the formation of microstructures, important analytical procedures to test the durability of concrete and a brief comparative study of the above.

2. MICROSTRUCTURE

2.1 The porous structure of concrete

Porosity can be defined as the volume of voids present in a porous material as a fraction of the total volume. Two types of voids can be presented in a porous material, discrete pores, and interconnected pores. Discrete pores have no influence on concrete permeability; however interconnected pores have a substantial impact (Kosmatka et al., 2011). According to most study permeability increases while capillary porosity increases, and also strength decreases with increasing porosity (Kosmatka et al., 2011; Powers et al., 1959; Li and Roy, 1986). Permeability shows a sharp decline once porosity drops below 30%, and it effectively reaches zero when the porosity of the cement paste falls to around 20%. Under de-percolated conditions, the permeability is approximately 10^{-14} m/s.

Table 1: The approximate amount of time needed for capillary pores to shift from connected to disconnected during the hydration process for moist-cured concrete (Powers et al., 1959)

Water-Cement (w/c) ratio	Degree of hydration	Required days
0.4	50	3 Days
0.45	60	7 Days
0.5	70	14 Days
0.6	92	6 months
0.7	100	1 year
> 0.7	100	Impossible

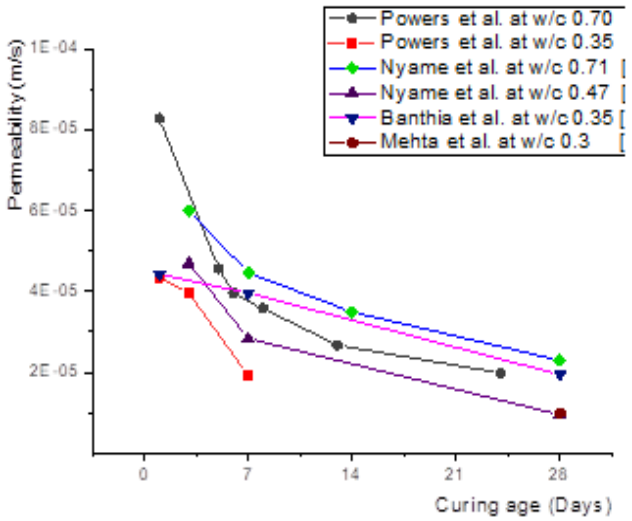

Figure 1: Comparison of permeability and curing ages with different w/c ratios reported by different authors (Ye, 2005)

Table 1 shows the time required for the transition of capillary pores from connected to disconnected during the hydration time of the cement based on the results of water permeability reported by (Powers et al., 1959). According to this finding, this transition takes place at about 20% of porosity. From the data of Table 1, the cement paste made with a water-cement ratio greater than 0.7 never becomes discontinuous. As a result, the water-cement ratio is a critical factor in the long-term durability of concrete. Indeed, the water permeability of cement paste reported by other researchers shows significant variations with (Figure 1) (Powers et al., 1959).

For example, the experimental results obtained by showed a contradiction with powers *et al.*'s result (Mehta, 1980). According to their experimental result, the de-percolation threshold of capillary porosity does not occur in cement paste with a water-cement ratio of above 0.30, even at ages up to one year. Similar results were obtained by a group researcher for the samples with a water-cement ratio of 0.35 and 0.47 respectively (Banthia and S. Mindess, 1988; Hughes and R. Amtsbüchler, 1986). Furthermore, test results obtained have shown that the permeability is largely dependent on several factors such as sample preparation, curing conditions (sealed or saturated), type of media used in permeability tests (N_2/O_2/water/other liquid solutions), the pressure used for the tests and, age of the sample (Banthia and S. Mindess, 1988; Hillel, 2012). Specially curing conditions play a major role in the permeability of pore structure. According to the experiments carried out by the degree of hydration is higher for the sample which is cured under saturated condition than sealed condition (Bentz, 1997). During the hydration of the sealed curing sample, empty pores can be developed. The deviation with powers *et al.* results were further tested and confirmed by Guang Ye with the help of a numerical simulation model and experiments (Table 2) (Powers et al., 1959; Ye, 2005). This indicate that the de-percolation of pores occurs at 5% porosity for the sample of w/c ratio of 0.3 and the degree of hydration of 0.68. As the results pore size distribution, critical pore diameter, and effective porosity are the key factors that control the water permeability (Ye, 2005).

Table 2: Degree of hydration, porosity, and permeability of concrete with the function of time concerning different water-cement (w/c) ratio (Ye, 2005).

W/c ratio	Age (days)	Degree of hydration (%)		Total porosity (%)		Effective porosity (%)		Measured permeability (m/s)
		Measured	**Simulated**	**Measured**	**Simulated**	**Measured**	**Simulated**	
0.4	3	45.1	45.6	33.2	32.1	22.2	29.1	6.42×10^{-12}
	14	64.1	64.8	29.1	26.0	19.3	23.5	4.48×10^{-13}
	28	-	72.1	22.1	21.0	11.3	16.8	9.00×10^{-14}
0.5	3	46.2	46.4	40.5	41.4	27.3	40.8	1.54×10^{-10}
	14	68.9	69.2	35.0	32.1	20.9	30.9	2.14×10^{-11}
	28	-	77.2	31.1	28.9	17.0	25.8	1.33×10^{-12}
0.6	3	47.3	48.2	45.7	46.0	33.7	45.5	4.61×10^{-10}
	14	73.6	73.8	41.5	40.2	26.0	39.1	7.61×10^{-11}
	28	-	84	39.5	36.5	23.0	34.2	1.82×10^{-11}

Porosity, pore size distribution, and means pore radius are key parameters in cementitious materials regarding microstructure. They are related to durability, ionic resistivity, fracture toughness, and flexural strength (Roy, 1988). The Hydration reaction of cement starts upon the addition of water. The heat generated by the hydration reaction eliminates along with water at the initial stage of hydration by creating some pores and through existing pores. Mainly there are four types of pores in cement-based materials, capillary pores, gel pores, macro-pores due to intentionally entrained air, and macro-pores due to insufficient compaction. The size of the pores varies from nanometre to millimetre where gel pores (1- 5nm) and capillary pores (5-50 nm) are smaller and air voids usually larger than 10 μm (Zhou, et al., 2019; Van Breugel, 1993). Generally, a high water-cement ratio increases porosity. Furthermore, alkali leaching can create more capillary networks as it expels water-soluble hydration products i.e., portlandite and alkali oxides. The connectivity of the pore can be expressed by Eq 01 (Ye and Van Breugel, 2009).

$$\text{Connectivity of pores}(\psi) = \frac{\text{Connected pore volume}}{\text{Total pore volume}} \quad (1)$$

The value of $\psi = 1$ means, all pores are connected, and if $\psi = 0$, no pore path goes from one side to the other side. The schematic diagram of the Porous Structure of concrete is given in Figure 2.

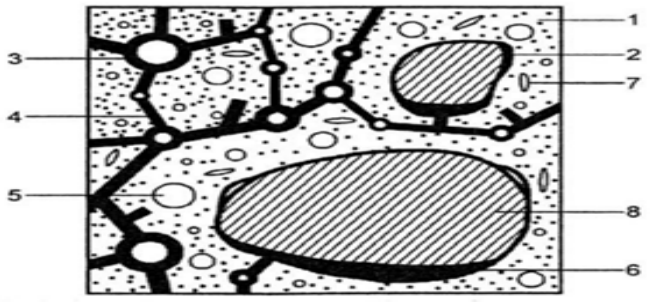

Figure 2: The schematic diagram of porous structure of concrete, 1-gel pores, 2-pores in the contact zone between aggregate grains and cement paste, 3-air opened pores, 4- capillary pores (Continuous), 5-closed off pores, 6- sedimentary pores, 7-microcracks, 8-aggregates grain (Bołtryk and Pawluczuk, 2010)

Porosity, critical pore size, pore-volume, and capillary porosity are considered as pore structure parameters. These parameters can be obtained by pore size distribution measured by the Mercury intrusion porosimetry (MIP) test. Among them, the critical pore size and capillary porosity are important on permeability (Zhang, 2008). The percentage of capillary porosity can be calculated by Eq 02 (Wang, et al., 2017).

$$\phi_c = \frac{V_1}{V_{Total}} \times \phi \quad (2)$$

where ϕ_c is the percentage of capillary porosity, V_1 is the volume of pores with sizes in the range of 10–10,000 nm (mL/g), ϕ represents the percentage of total porosity V_{Total} is the total volume of concrete sample.

2.2 Effect of hydration on porosity

The porosity of concrete based material reduces with the hydration process as hydration products fill the spaces. But it is notable that in concrete, the volume proportion of large pores significantly reduce, whereas the small pores (<100Å) significantly increase (Van Breugel, 1993). At the early stage of the hydration volume of large pores reduce due to the formation of hydration products in the large pores. But in small pores, the formation of hydration products takes place later. When the larger voids are filled, additional hydration can affect the whole pore size distribution. It has been experimentally proven that the profile of the pore size distribution affects the degree of hydration in the cement materials (Hu, 2004). The sample distribution of the pore network with different hydration time is given in Figure 3. Where water/air space is represented by white areas and solid phase (un-hydrated cement and hydration products) is represented by black areas.

Figure 3: Sections of bulk-paste with a water-cement ratio of 0.5. Where (a) Initial stage of hydration; (b) After 3 days of hydration, and (c) After 10 years of hydration (Lichtner, et al., 2018)

The addition of pozzolanic materials like calcined clay, fly ash, nano-silica, etc., make the microstructure of concrete denser. Due to the densification process, the capillary pore becomes constrained and largely disconnected and tortuous (Dhandapani and Santhanam, 2020).

2.3 Permeability

Concrete structures that are exposed to the unfavourable environmental conditions should have low permeability for the extended service life. It is well known that fluids migrate easily through high permeable materials. The permeability of substances made by concrete also depends on the degree of hydration, w/c ratio, and the period of moist curing. A sufficient period of moist curing and a low w/c ratio make a concrete low permeable nature (Kosmatka, et al., 2011). This attribute is attained by the reduction of porosity caused by good hydration as mentioned in section 2.2. Water leakage was not seen in samples with a water-cement ratio of 0.50 or less that had been moist-cured for seven days. Mortar disks were made with a higher water-cement ratio than 0.5 subjected to leakage (McMillan and Lyse, 1929). Leakage was also reduced for the sample that had been adequately moist cured. Low w/c ratio and appropriate moist curing during sample preparation have an important role in the durability of concrete, according to experimental results acquired by various research.

Several concrete admixtures are still being investigated to reduce the permeability. Addition of polyvinyl alcohol fibres (PVA) in a suitable amount can reduce the water permeability for a certain level. Specially application of PVA fibres has been studied by several researchers, that is used to formulate the Engineered Cementitious Composite (ECC) (Pakravan, et al., 2017). The micro/ Nano polymer fibres that reduce the water permeability have tendency to absorb the water and swell. This feature account for the permeability reduction in concrete. Aside from polymer fibres, addition of superabsorbent polymer/rubber also reduce

the water permeability in an adequate level. These polymer additives absorb the water that penetrate through the pores in concrete, swell and seal the path. However, to achieve high permeability, the delivery strategy of these swelling polymers will need to be enhanced in the future (Natkunarajah, et al., 2023). Diffusivity refers to the flow of water dissolved ions through a porous material. Decreased permeability and diffusivity make concrete better resistance to the passage of chloride ion, freeze-thaw cycles, and other types of the chemical attack. The transport properties are affected by the size of the molecules or ions that are transported through the concrete, the valence of the ions, and the viscosity of the fluid (Kosmatka, et al., 2011).

2.3.1 Calculation of permeability

Pore volume directly influences the permeability of porous materials. There are several direct calculation methods that have been reported previously to measure the permeability (Lichtner, et al., 2018). Darcy's classic equation (Eq 03) is well recognized to calculate the permeability of porous materials (Lichtner, et al., 2018).

$$Q = \frac{Ak\ \Delta P}{\mu\ \Delta x} \tag{3}$$

Where:

Q - Volumetric flow rate of fluid through the medium

A- Area of the medium

K - Permeability of the medium

μ - Dynamic viscosity of the fluid

ΔP - Applied pressure difference

Δx - Thickness of the medium

Direct calculation of permeability through the experiment is a time-consuming method, especially for the low permeability concrete. The permeability of cementitious materials can be better understood using computational models and mathematical equations.

Katz-Thompson equation (Eq-04) and the Carman-Kozeny relationship (Eq 05) are generally used in modelling studies (Katz and Thompson, 1986; Carman, 1939). Water permeability can also be correlated with MIP data using similar models. However direct application of Katz-Thompson equation for the permeability calculation in a concrete system always will not provide appropriate results (Tumidajski and Lin, 1998). As a result, a modified version of the Katz-Thompson equation is being used by various researchers to tackle this problem (Hu, 2004). According to the Carman-Kozeny model, the geometrical features of pore spaces can be used to estimate the permeability (k) of cement paste.

$$k = \frac{1}{226}\ l_c^2\ \frac{\vartheta}{\vartheta_0} \tag{4}$$

Where:

k – Permeability

lc - Critical pore diameter

ϑ - Electrical conductivity of the sample

ϑ0 - Electrical conductivity of the pore solution in the sample.

$$k = -\frac{p(V_{pore} / S_{pore})^2}{2\beta} \tag{5}$$

where:

k – Permeability

p – Porosity

V_{pore} – Volumes of pore space

S_{pore} - Surface area of pore space

β - Tortuosity of the transport route in the cement

Spore - Surface area of pore space

β - Tortuosity of the transport route in the cement

3. DURABILITY

Attention towards durability problems arises when the materials get damage at the earlier stage. Sometimes the material damages do not require an immediate safety issue. However, these damages lead to large structural damage progressively. This may lead to larger damage to the structure as well as cause a large economical loss. Deterioration of concrete structure can be caused by physical conditions, chemicals, and mechanical factors. Most concrete durability failure mechanisms are influenced by the availability of moisture. Failure processes generally involve two steps. At the initial stage, harmful solutions containing hazardous ions or dissolved gasses are transported through the capillary pores of the cementitious structure to the reactive sites (Chloride ion reach the reinforcement bar, sulphates ion transport to aluminates) and then they induce chemical/physical degradation mechanisms.

In many cases, corrosion of reinforced steel bar-related structural damages seriously affects the durability of concrete structure (Zongjin, 2011). Therefore, it is important to stand against the imbibe of fluids (low permeability) for the high durability of concrete (Kosmatka, et al., 2011). This implies that the design of concrete must be with lower water content and a low w/c ratio to increase the lifetime of the cementitious structure. Additional to water content sufficient curing time is also important. It happens because pore volume reduces with increased hydration reaction as mentioned above (See section 2.2). Increased curing time also reduces the permeability of concrete.

Durable material is favourable when it serves without major repair before its predicted service life. It must not be estimated that the preparation of durability is a substitution for maintenance. Sometimes, proper maintenance and regular inspection are necessary for the structure which is designed for high durability.

There have been numerous studies conducted to address the issues of durability. Most previous studies have focused on isolated deterioration mechanisms such as reinforcement corrosion, freeze–thaw damage, alkali–aggregate reaction, carbonation, portlandite leaching, and sulphate attack. In practice, however, concrete structural failure typically results from the combined action of multiple factors. Therefore, numerous researchers have modified their work from an individual factor to the combined effect of multiple factors. These studies propose ideas for increasing the service life of cementitious materials depending on their durability.

The durability of cementitious materials depends on a range of factors which include, the curing type, the Curing period, the water-cement ratio, the type of cement and aggregates used, porosity, carbonation, and penetration of harmful materials (Tang, et al., 2015). Among them, permeability and porosity play a significant role as it dominates the rate of transport of harmful molecules. The size of most ions and gasses that are harmful to the concrete is below the size of the gel pores (Gowripalan, et al., 1990).

3.1 Continuity of water in capillary pores

The arrangement of pores in unsaturated cementitious materials is partly continuous and partially discontinuous as mentioned above (see chapter 2.1). Continuous pores form a network structure as shown in Figure 2 and water-filled continuous pores allow the transport of harmful ions. The water continuity ηw can be described by the equation (Eq 06) given below.

$$\eta_w = \frac{N_w}{N_{sat}} \tag{6}$$

N_w: Number of capillary channels available for ionic transport at a certain saturation state.

N_{Sat}: Number of capillary channels available for the ionic transport at a

complete saturation state.

In a complete saturation state, all the connected pores are filled with water. At this condition, $N_w = N_{sat}$, and η_w reaches one ($\eta_w = 1$). When the water saturation decreases, the value of N_w decreases, and ultimately, the value of η_w decreases. The water phases in cementitious materials can be categorized into gel water, capillary water, and non-evaporable water (Powers, 1945). During the movement of the water molecule, one part of the capillary water is absorbed on the pore wall physically. Remaining free water molecules correspond to ionic transport. The capillaries in unsaturated cementitious materials may be fully water-filled or partially water-filled or completely drained. In a drained pore, there must be a thin film of water adsorbed on the pore wall (Zhang and Ye, 2018). The thickness (t) of the water film is based on the relative humidity (Rh) of the porous system. Ingress of harmful ions like chloride is viable in completely and partially water-filled pores but it is hard in drained pores (Zhang and Ye, 2018).

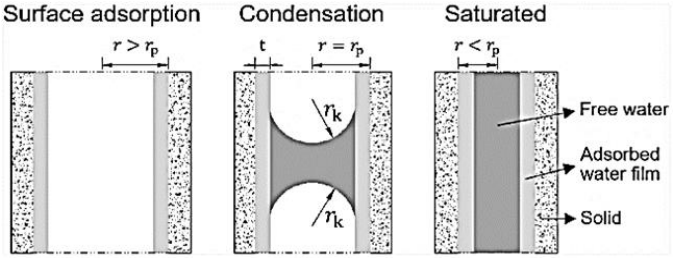

Figure 4: Nature of water distribution in a porous material at a certain Rh value (rp=rk+t) rk - Kelvin radius, rp - pore radius, t - thickness of water film (Krivenko, et al., 2014)

The nature of water continuity in a pore is illustrated in Figure 4. According to Kelvin's law, the radius (r_k) of a meniscus depends on the RH value. The pores with radius $r < r_p$ ($r_p=r_k+t$) are filled with water, whereas the pores with radius $r > r_p$ are drained (Thin water film remains on the wall). Therefore, in low Relative humidity and lower water continuity η_w, a lower degree of water saturation (S_w) has resulted. The relationship between η_w and S_w is remarkably influenced by the pore structure. Porosity, pore size, pore connectivity, and tortuosity are all parameters of the pore system employed in mass transport research (Zhang, et al., 2019). Furthermore, the multiple porous systems with a range of changing porosity (other properties are identical) exhibit the same water continuity η_w and moisture distribution at a given degree of water saturation Sw. In this situation, the porosity does not influence the η_w-S_w relationship (Zhang, et al., 2019). While considering pore size, a finer pore size distribution leads to the reduction of water continuity (η_w) for a system that has a certain degree of water saturation (S_w). The reason may be the water loss in finer pores occur easily and the pores become drained. In this situation, η_w can be sensitive to water loss. Anyhow, the effect of the pore size on η_w is significant at higher saturation levels but becomes weak at lower saturation levels (Zhang, et al., 2019). Not only that, porosity include both connected and discrete pores, but S_w is higher into the interconnected pores while low into the discrete pores. Continuity of water in capillary pore play significant role in chloride and sulphate attack as it eases the penetration of these substances.

3.2 Sulphate attack

Numerous research is being carried out regarding the sulphate attack as it plays a significant role in concrete durability (McCarthy and Dyer, 2019; Ideker, et al., 2019). The serious effect of sulphate attack has led to the production of sulphate resistant cement. Portland cement type V (ASTM C150) is such type of cement, and the maximum amount of tricalcium-aluminate included is 5% (Bogue's composition) (Stutzman and Leigh, 2010). Sulphate attack in concrete mostly occurs externally (External sulphate attack), nevertheless, internal sulphate attack also occurs due to the delayed ettringite formation (Alexander et al., 2013). Cement contains a significant amount of Tricalcium aluminate (C_3A). The existence of C_3A in cement is undesirable because it provides little/nothing to the strength of cement structure (Shetty, 2000). When the concrete structure is attacked by sulphate, it forms calcium sulfoaluminate (Ettringite) which disrupt the concrete health (Neville and Brooks, 1987). The formation of expansive ettringite during sulphate attack is represented by the following ionic equation (Eq 07).

$$6\,Ca^{2+} + 3SO_4^{2-} + 2Al(OH)_2^{-} + 4OH^{-} + 26H_2O \longrightarrow 3CaO.Al_2O_3.3CaSO_4.32H_2O \quad (7)$$

Ettringite is unstable at a low pH level (below 11.5-12) where it could be decomposed to form gypsum. Ettringite also can be formed with the reaction of gypsum ($CaSO_4$). Furthermore, incoming sodium sulphate (Na_2SO_4) reacts with portlandite ($Ca(OH)_2$) and produce gypsum ($CaSO_4.2H_2O$). Formed gypsum is expansive and may turn ettringite in the presence of aluminates. Ettringite can swell and shrink by gain and loss of water. Expansion of ettringite can create a micro crack in concrete (Kosmatka, et al., 2011). But it is doubtful on this behaviour for the damage to hardening concrete (Brown and Taylor, 1999). Nevertheless, the formation of ettringite by sulphate attack on hardened concrete can lead to severe damage.

The experimental results regarding the effect of sulphate attack on C_3A reveal that mortar prepared from C_3S and C_2S showed a very good resistance, whereas samples containing C_3A were badly damaged within a very short time. The expansion of specimens containing C_4AF was lower than for mortars containing C_3A (Monteiro and Kurtis, 2003). The reaction of sulphate in dense microstructure to ettringite can leads to expansion and the formation of micro cracks, especially around aggregates (Brown and Taylor, 1999).

The presence of portlandite increases the formation of ettringite as it is converted into $CaSO_4$. The addition of pozzolanic materials can convert the portlandite into secondary C-S-H gel. The high solubility of aluminium in the absence of portlandite after a pozzolanic reaction, can result in a transport of aluminium over longer distances and therefore ettringite can preferentially be formed in large empty pores (Damidot and Glasser, 1993; Brown and Taylor, 1999). Therefore, it can be said that the incorporation of pozzolanic raw materials can reduce the formation of ettringite and thus escalate the resistance to sulphate attack. Considerable improvement in sulphate resistance can be obtained by using low C_3A content cement and addition of pozzolanic materials especially fly ash (Monteiro and Kurtis, 2003). Additional to C_3A content present in the cement, sample preparation also effects the sulphate attack. Especially higher w/c ration can increase the risk of sulphate attack (Monteiro and Kurtis, 2003).

With any source of sulphate, in the presence of carbonate/bicarbonate and silicate ions, the formation of thaumasite ($CaSiO_3.CaCO_3.\ CaSO_4.15H2O$) can occur (McCarthy and Dyer, 2019). A low temperature of less than 10°C favour the formation of thaumasite. Thaumasite plays an important role in sulphate attack as it causes consequent loss in strength than ettringite. The formation of thaumasite can be expressed in Eq 8.

$$Ca_3Si_2O_7.3H_2O\,(C\text{-}S\text{-}H) + 2CaSO_4.2H_2O + 2CaCO_3 + 24H_2O \longrightarrow$$

$$Ca_6[Si(OH)_6]_2(CO_3)_2(SO_4)_2.24H_2O\,(Thaumasite) + Ca(OH)_2 \quad (8)$$

Thaumasite formation is very detrimental because it leads to the breakdown of C-S-H gel, portlandite, C-A-H, hydrated aluminate phases, and ettringite of concrete. Thereafter, significant strength loss of hardened concrete can be noticed. The indication of its characteristic destruction is to transform the surface of the concrete into a white pulpy mass (Profile, 2001).

In addition to ettringite formation and Thaumasite related sulphate damage, other types of sulphate attacks were also reported (Brown, 2002). Such types include Delayed ettringite formation; Physical sulphate attack related to the crystallization of sulphate containing salts; and Sulphate attack connected with the formation of AFM phases (alumina-ferric oxide-monosulphate) (Brown, 2002).

3.3 Alkali aggregate reaction (AAR)

Alkali aggregate reaction (AAR) in cementitious structure is the reaction of alkali contents in the pore solution with alkali sensitive compounds of aggregates. AAR can be classified into two types, alkali-carbonate reaction (ACR) and alkali-silica reaction (ASR). Alkali-carbonate reaction involves the reaction of alkalis with effective minerals from dolomitic limestone aggregate whereas the ASR involves the reaction of alkalis with amorphous silica in the aggregates.

Testing methods for AAR are: "Autoclave test method, accelerated mortar bar method (ASTM C1260), Quick testing methods (ASTM C289), Mortar bar trial (ASTM C227), Rock cylinder method (ASTM C586), testing the concrete prism (RILEMAAR-3), chemical constriction test, stiffness damage trial, gel fluorescence testing compound activation energy measurement method and, Dynamic modulus" (Yamada, 2014; Knudsen, 1985; Sanchez, et al., 2014; Liu and Mukhopadhyay, 2014). The degree of AAR is influenced by the type of reactive silica, the amount of reactive silica, and the amount of alkali contents in the cement.

The degree of AAR is influenced by the amount of water present, alkali

contents, Porosity of cementitious material, and the temperature. Therefore, the selection of suitable cement, suitable aggregates and proper sample preparation can reduce AAR. Addition of a significant amount of pozzolanic materials can reduce the AAR by converting alkali into secondary C-S-H gel (Tang, et al., 2015). Furthermore, it was experimentally proven that addition of lithium nitrate in cementitious material reduce the effect of AAR (Leemann, et al., 2014). This makes hydration products denser and influences the chemical composition and physical property of hydration products.

AAR has a negative impact in many cases, but positive effects have been observed in some investigations at earlier stages of hydration:

- The mortar with activated dolomite aggregates exhibited considerably higher compressive strength compared with limestone aggregates because of the ACR. This result was due to the formation of a new phase of the Mg–Si–Al network in the interfacial transition zone (ITZ). This phase provides better interlocking between cement and aggregate grains (Štukovnik, et al., 2014).
- Addition of activated alumina to the alkali-activated cement had a positive impact on regulating the structure formation process in the ITZ. Moreover, it reduces the expansion to an acceptable level (Krivenko, et al., 2014).
- Formation of Alkali-silica gel and secondary ettringites was observed through the scanning electron microscope for the concrete sample blended with alkali reactive brick aggregates (Bektaş, 2014). However, the strength property of this formulation was not affected by the addition of alkali reactive brick aggregates.

3.3.1 Alkali-Carbonate Reaction (ACR)

Alkali carbonate reaction denotes the dolomite in the dolomitic aggregates reacts with OH^- and produce $Mg(OH)_2$ (brucite), $CaCO_3$ (calcite), and CO_3^{2-} (Carbonate) as shown in Eq 09. Here formed carbonate ion reacts with portlandite in concrete and produces $CaCO_3$ as shown in Eq 10.

$$CaMg(CO_3)_2 + 2OH^- \longrightarrow Mg(OH)_2 + CaCO_3 + CO_3^{2-} \quad (9)$$

$$CO_3^{2-} + Ca(OH)_2 \longrightarrow CaCO_3 + 2OH^- \quad (10)$$

Volume reduction in solid phase down to 5.1% and volume increment up to 10.2% can be described by Eq 09 and Eq 10 respectively. The depletion of dolomite is called a dedolomitization reaction (Kosmatka, et al., 2011). The formation of brucite and the dedolomitization reaction can lead to considerable expansion. The following experimental methods are widely used to identify the potential of ACR (Farny and S. H. Kosmatka, 1997).

- Petrographic examination (ASTMC295)
- Rock cylinder method (ASTMC586)
- Concrete prism test (ASTMC1105)
- Chemical composition method (CSAA23.2-26A)

Chemical and physical properties of ASR and ACR products are different and organic alkali (tetramethylammonium hydroxide-TMAH) can be used to identify the effect of ACR which could be distinguishable from ASR. TMAH react with dolomite present in the carbonate rock and increase in volume. However, it does not react with the components that can undergo an ASR reaction. Indeed, ACR is relatively rare since the type of aggregates vulnerable to this reaction is generally unsuitable to be used in concrete due to the strength perspective (Kosmatka, et al., 2011).

3.4 Chloride attack and corrosion of steel bar

Chloride-induced corrosion of reinforced steel bar is a key concept regarding the durability of concrete. Several studies are still underway to find an effective admixture or mix-preparation method for reducing or preventing steel corrosion in concrete structures. The high alkaline nature protects reinforced steel bars by forming a passive film (Natkunarajah, et al., 2021). Penetration of substances such as chloride ion and CO2 gas reduce the pH level of concrete matrix. The stability of the passive film on steel bars begins to deteriorate when the pH of the concrete falls below 11.5. When it falls below 10, the passive film's protective action is completely lost (Zuo, et al., 2017). This de-passivation is caused by the reduction of [Cl-/OH-] molar ratio and at this condition activity of Cl- ion exceed the activity of OH- ion. To express the Chloride threshold level, represent the total chloride content concerning the total cement weight is a better way than representing as [Cl-/OH-] molar ratio (Natkunarajah, et al., 2021). When this critical value is attained and in the presence of oxygen and moisture, corrosion of the re-bar initiated. Corrosion products are approximately a six-time higher volume than iron. Therefore, cracking and spalling occur and hence it shortens the shelf life of the concrete structures (Tutti, 1982).

The corrosion of the re-bar is an electrochemical process. This process begins when the chloride corrosion threshold of concrete is attained, and an electric cell is formed along/between the steel bars (Kosmatka, et al., 2011). The chloride corrosion threshold is attained when the water-soluble chloride becomes about 0.15% by mass (Kosmatka, et al., 2011). The schematic diagram of the corrosion mechanism is given in Figure 5. After the initiation of corrosion, the corrosion rate is dominated by the moisture content, electrical resistivity/conductivity, and oxygen migrating rate through the concrete to the steel. Chloride ions present in the concrete react with iron to form soluble iron chloride and that translocate to the concrete matrix and converted into iron oxide later.

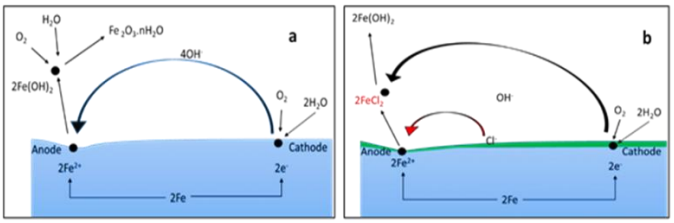

Figure 5: (a) Schematic diagram of the corrosion mechanism of concrete reinforced steel bar Schematic diagram of the corrosion mechanism of concrete reinforced steel bar, (b) corrosion mechanism with chloride ion.

The anodic and cathodic reaction can be described as following in the Equations Eq 11 to Eq 14 (Shetty, 2000).

Anodic reaction:

$$Fe \longrightarrow Fe^{2+} + 2e^- \quad (11)$$

$$Fe^{2+} + 2(OH)^- \longrightarrow Fe(OH)_2 \quad (12)$$

$$4\,Fe(OH)_2 + 2H_2O + O_2 \longrightarrow 4\,Fe(OH)_3 \quad (13)$$

Cathodic reaction:

$$4\,e^- + O_2 + H_2O \longrightarrow 4(OH)^- \quad (14)$$

Chloride ion acts as a catalyst for the corrosion of the steel bar. The action of Cl- ion in steel corrosion is described in Figure 5 (b). The chloride diffusion capacity of concrete could be measured by using the chloride diffusion coefficient (Zhang and Ye, 2019). The passage of chloride iron depends on the moist level and moist distribution of the concrete. Nernst-Einstein equation based computational model was recently developed to predict the chloride diffusion coefficient (Zhang and Ye, 2019). The chloride diffusion coefficient depends on many factors such as moist content, critical relative humidity, pore's structure, and water continuity (see section 3.1), and conductivity of concrete matrix (Zhang and Ye, 2019). Porous materials with lower pore diameters (less than 30 nm) have a bigger impact on the Relative-chloride-diffusion-coefficient and degree of water saturation than porous materials with larger pores (greater than 100 nm) (Zhang and Ye, 2019).

4. Test Methods

There were numerous test methods that have been carried out by many researchers to analyse the microstructure and durability of concrete. FT-IR spectroscopy, scanning electron microscope (SEM) investigation, X-ray powder diffraction, X-ray fluorescence spectroscopy, and Thermo gravity analyser (TGA) are widely used by researchers in concrete-related studies. Here we focus on other important analytical methods.

4.1 Mercury intrusion porosimetry (MIP)

MIP method is a traditional method used to analyse the pore size distribution and connectivity of concrete samples (Rootare and Prenzlow, 1967). It comprises a wide range of pore sizes in the hardened cementitious materials, and it is a quick measurement technique. To take measurements, the pressure will be applied with gradual increment to inject the mercury into the pores and at the same time intruded volume of mercury will be measured. The specific area can also be calculated using this method (Rootare and Prenzlow, 1967). Pore diameter (d) with respect to each pressure step, can be calculated from the Washburn equation (Eq 15).

$$p = \frac{4\gamma\cos\theta}{d} \quad (15)$$

Where,

p - Injection pressure

d- Pore diameter concerning injection pressure.

γ - Surface tension of mercury

θ- Contact angle between solid and mercury

Although, the pore distributions obtained by MIP measurements are not an actual description of the porous structure. Because the whole volume of a pore is allocated to its diameter on the surface of the sample. If the biggest diameter of a pore is on the surface of a specimen, this can give a correct tally of volume versus pore diameter using Eq 15. Because of this effect, the volume of pores is characterised as smaller than the actual size. The results obtained by SAXS (Small-angle X-ray scattering) provided enormous surface areas than obtained by MIP and gas sorption.

4.2 Nitrogen adsorption method

The nitrogen adsorption method is another method to calculate the total porosity and internal surface area of concrete. The nitrogen adsorption method can cover a more specific area that could not be detected by the water vapour adsorption method (Mikhail, et al., 1964). By the nitrogen adsorption method, pore radii between 1 nm and 60 nm can be measured. This method depends on the quantity of nitrogen adsorbed or desorbed to the applied pressure. The test results depend on the moist in the sample and so, it changes on drying methods (Juenger and Jennings, 2001).

Procedure:

Dry the cured sample with a suitable drying method (vacuum drying/oven drying method) to remove the moisture in the concrete. Then grind them in CO2 free atmosphere to the appropriate size (50 mesh/ 0.297 mm). Then measure the nitrogen sorption at low temperature (77 K) (Zhou, et al., 2019).

Then the specific surface area is calculated through the BET method. BET method is another widely used technique to determine the specific surface area of the porous solid materials. The following equation (Eq 16) is applied in this method.

$$\frac{p}{v.(p_0 - p)} = \frac{1}{v_m . C} + \frac{C - 1}{v_m . C} \times \frac{p}{p_0} \quad (16)$$

Where:

v – Volume of the adsorbed substance (nitrogen or water)

p – Equilibrium pressure

p_0 – Saturated pressure

v_m - Volume of the adsorbent that is adsorbed on the sample in case of monolayer adsorption.

C – Constant.

Here constant C describes the interaction between the sample and adsorbed gas, where a greater value of C reflects a greater interaction. This method is usually applied to determine the specific surface area of cement pastes. Indeed, if interpreted properly, useful information about the pore structure can be gained. Besides the nitrogen adsorption method, the water vapour adsorption method is also widely used to analyse pore distribution.

4.3 X-ray micro tomography (micro-CT)

The application of micro-CT in concrete is an emerging technique to analyse the pore size distribution and pore connectivity in concrete. MIP method is an indirect measurement of pore analysis, but the 3D structure of internal pore networks can be created by micro-CT with a resolution of 1-5 µm per volumetric pixel (Ranachowski, et al., 2015). The same technique used in medical computed axial tomography (CAT) scans machine is used in micro-CT. Nevertheless, micro-CT has sufficient spatial resolution with the combination of extremely bright, monochromatic synchrotron radiation with high-quality optics and x-ray detection. Furthermore, the micro-CT is applied in the studies of internal fracture, sulphate attack, and cement hydration.

4.4 Sulphate attack test

An experimental procedure for external sulphate attack is a very simple but time-consuming method. For the normal test procedure, cured concrete sample (Minimum 28 days) is immersed into a sulphate solution of Na / K/ Mg / Ca at constant temperature. The concentration of sulphate is usually taken as 5%. After a certain time of exposure, a sulphate solution may be replaced and the physical properties of the sample Such as dimension change, strength, visual appearance, etc. will be checked. However, ASTM C1012 is the standard test method for determining sulphate attack. Nevertheless, it consumes 6-12 months for the measurement. The test procedure of ASTM C1012 is given below (ASTM, 2012).

Procedure:

Prepare mortar prism (25×25×285mm), with a gauge length of 250 mm and enough number of mortar cubes. After that Immediately, place the prisms and cubes in large polyethylene bags, seal them, and submerge underwater at 35 °C. After 24 hours, remove the moulds and transfer to a limewater bath at 23 °C until achieving a compressive strength of 20 MPa from the average of 2 mortar cubes (usually it takes about 2-3 days). Measure the initial length and weight. After the initial measurement transfer the sample into a sodium sulphate solution (5% Na2SO4) at 23°C. Thereafter, measure their length and mass change according to the schedule provided in ASTM C1012 and renew the solution after each measurement. There are also some suggested methods for speeding up the sulphate attack (Aguayo, et al., 2020). These methods can be used to avoid the inconvenient ASTM C1012 method, which takes longer to complete.

4.5 Standard Test Method for Half-Cell Potentials of Uncoated Reinforcing Steel in Concrete

This method is the standard method to determine the corrosion of uncoated steel bar in concrete (ASTM C 876/09) (ASTM 2009). The region act as Anodic during corrosion is more negative potential while the cathodic region is more positive electrical potential. By using this potential difference, the anodic and cathodic region can be detected by measure the potential on the surface (ASTM 2009).

Significance and use:

- This test method is suitable for in-service evaluation and research.
- This test method applies to members regardless of their size or the depth of concrete cover over the reinforcing steel.
- This test method may be used at any time during the life of a concrete member.
- The results obtained by this test method shall not be considered as a means for estimating the structural properties of the steel or reinforced concrete member.

The positive electrical connection is made with a reinforced steel bar, and a negative electrical connection is made with the half-cell. The half-cell consists of copper sulphate solution and copper rod. Due to the high resistivity of concrete, a high impedance voltmeter is essential. Wetting solution is applied on a concrete surface (if necessary) and measurement of the voltmeter will be taken. The measurements will be carried out in a pre-determined pattern. Test results provide the corrosion probabilities/activity but not the location of corrosion activity (ASTM

2009).

4.6 The rapid chloride permeability test (RCPT-ASTM C 1202-12)

Rapid chloride permeability test is widely used to measure the resistance of concrete to chloride ions penetration. The contribution of chloride ion in corrosion of steel bar plays a significant role, therefore a measurement of chloride permeability is important regarding the durability of concrete. This test method was primarily developed for a fast test to calculate the chloride diffusion coefficient, but later it is found as a measure of electrical resistivity. ASTM C 1202 method is widely used as quality control (Concrete Institute of Australia, 2015).

The concept of RCPT is based on ion mobility. Here chloride ions are forced into concrete by applying electric potential on the concrete surface and ion mobility can be calculated using Eq 17.

$$\mu = \frac{x}{t} \cdot \frac{dE}{dx} \tag{17}$$

Where:

μ - Ionic mobility (cm^2/ V.s)

x – Distance (cm)

t – Time (s)

dE/dx – Strength of electric field (V/cm)

Procedure:

The dimension of the test concrete specimen is 100 mm in diameter and 50 mm thick according to ASTM 1202-12 (ASTM, 2012). Coat the curved surface of the specimen with epoxy and allow it to dry. After that keep the specimen in a vacuum chamber for 3 hours to eliminate the air. Then allow the specimen to saturate in a vacuum for 1 hour and soak in water for 18 hours. Fill the negative side of the test cell with a 3% NaCl solution and the positive side of the test cell with 0.3N NaOH solution. After that place the specimen in the test device. Then apply a 60-voltage direct current for 6 hours. Take the reading every 30 minutes. The amount of coulomb passed will be calculated for the respective reading. After calculating the amount of charge passed in coulomb, the values will be compared to chloride ion permeability as given in ASTM C1202-10 that is shown in Table 3.

Table 3: Chloride ion permeability based on charge passed (Kumar et al., 2020)

Chloride ion permeability	Charge passed (Coulombs)
High	>4000
Moderate	2000 – 4000
Low	1000 – 2000
Very low	100 – 1000
Negligible	< 100

RCPT is accepted as a major test for chloride ion penetrability in concrete, but it does not exactly represent actual conditions that the concrete experience in the field. There is no condition where concrete is exposed to a 60 V electric potential. RCPT measures the resistivity (Resistance = Voltage/Current) of concrete, but resistivity and permeability have a significant relationship.

5. Conclusion

This review has covered concrete microstructure analysis, which contributes to concrete durability, as well as several significant test procedures that are commonly used to predict concrete durability. The microstructure of concrete, particularly its permeability and porosity, has a significant impact on its durability.

Interconnected pores present in the concrete play as a controlling factor for the ingress of harmful compounds that affect the durability of concrete. To increase the durability of concrete structure permeability of harmful substances (e.g. Cl^-, CO_2, SO_4^{2-}) must be controlled and the concrete matrix must be a high alkaline nature. Permeability is directly depending on the porosity of the concrete. A lower w/c ratio and adequate curing/hydration are the factors that must concern during the sample preparation to reduce the porosity. The degree of hydration can be affected by curing conditions. The degree of hydration is higher for the sample which is cured under saturated condition than sealed condition.

Additionally, additives like polymer fibres and swelling polymers might clog the porous network and reduce permeability. Permeability can also be reduced by minimising the porosity, with the addition of pozzolan. Addition of pozzolanic materials (Fly ash, Meta kaolin, Silica fume, Calcined clay and so on) interfere with the hydration reaction of cement and reduces the porosity for a certain extent. The pozzolanic materials convert soluble portlandite (leach out by water) into secondary C-S-H gel and increase concrete durability by providing additional strength and reduce the capillary pores. Furthermore, some pozzolans such fly ash shows excellent chloride resistant capacity. The environmental factors such; alkali leaching can increase the porosity of concrete and that can increase the water continuity. This feature can reduce the durability of concrete.

Apart from the microstructure of concrete, external factors such as Sulphate attack, Chloride attack, carbonation, and AAR play an important role in the durability of concrete. Specially Cl^- and CO_2 gas reduces the pH level of concrete Which leads to the corrosion of reinforcement. Regular health monitoring (mainly the pH value) is essential for the in-service concrete structure. Non-destructive methods, such as optical pH sensors, fluorescence-based pH sensors, piezo-electric stress sensors, and chemical sensors, must be developed with high precision and be able to last long periods of time in a concrete environment.

The microstructure of concrete can be analysed by instrumental analysis such as FT-IR spectroscopy, SEM investigation, X-Ray de-fraction, Thermo gravity, etc., and by experimental techniques such as MIP, a nitrogen adsorption method, and Micro-CT, etc. The effect of sulphate attack is very significant in concrete as it damages the C-S-H gel by Thaumasite formation reaction.

A further detailed investigation is needed regarding AAR as some experimental results revealed that AAR has beneficial effects. Therefore, it is suggested that controlled alkali-aggregate reactions can improve the structural properties of concrete. Reaction and changes occurred by external chemicals and physical substances to the concrete are a very slow process. Most researchers use accelerated test techniques and computational predictions in concrete-related studies since getting data and analysing them takes more time.

Conflicts Of Interest

The authors have no conflicts of interest regarding the publication of this paper.

Acknowledgement

We gratefully acknowledge the Accelerating Higher Education Expansion and Development (AHEAD) under the DOR Grant (Grant No.27) for the financial support.

References

Aguayo, F., Funez, O. J., Drimalas, T., Folliard, K. J., Lute, R. D., 2020. An alternative method to evaluate the sulphate resistance of cementitious binders. In External Sulphate Attack – Field Aspects and Lab Tests Pp. 93–105. Springer. https://doi.org/10.1007/978-3-030-XXXX-X_7

Alexander, M., Bertron, A., De Belie, N. 2013. Performance of cement-based materials in aggressive aqueous environments (Vol. 10). Springer. https://doi.org/10.1007/978-94-007-5413-3

American Society for Testing and Materials. 2009. ASTM C 876/09: Standard test method for half-cell potentials of uncoated reinforcing steel in concrete. Annual Book of ASTM Standards (Vol. 91, Reapproved 1999, Pp. 1–6. ASTM International.

Arandigoyen, M., and Alvarez, J.I., 2007. Pore structure and mechanical properties of cement-lime mortars. Cem. Concr. Res., 37 (5), pp. 767–775. doi: 10.1016/j.cemconres.2007.02.023.

ASTM. 2012. Standard test method 1202-12: Electrical indication of concrete's ability to resist chloride ion penetration. Annual Book of ASTM Standards, 4, 7. ASTM International.

ASTM. 2012. Standard test method for length change of hydraulic-cement

mortars exposed to a sulfate solution. ASTM International. https://www.astm.org

Banthia, N., Mindess, S. 1988. Permeability measurements on cement paste. MRS Online Proceedings Library Archive, 137. https://doi.org/10.1557/PROC-137-321

Basheer, L., Kropp, J., and Cleland, D.J., 2001. Assessment of the durability of concrete from its permeation properties: A review. Constr. Build. Mater., 15 (2–3), pp. 93–103. doi: 10.1016/S0950-0618(00)00058-1.

Bektaş, F., 2014. Alkali reactivity of crushed clay brick aggregate. Construction and Building Materials, 52, 79–85. https://doi.org/10.1016/j.conbuildmat.2013.10.053

Bentz, D. P., 1997. Three-dimensional computer simulation of Portland cement hydration and microstructure development. Journal of the American Ceramic Society, 80(1), 3–21.

Bołtryk, M., Pawluczuk, E., 2010. Properties of recycled aggregate concretes modified by asphalt paste. In Proceedings of the 10th International Conference: Modern Building Materials, Structures and Techniques (p. 49). Vilnius.

Brown, P. W., 2002. Thaumasite formation and other forms of sulfate attack. Cement and Concrete Composites, 3(24), 301–303. https://doi.org/10.1016/S0958-9465(02)00037-7

Brown, P. W., Taylor, H. F. W., 1999. The role of ettringite in external sulfate attack. In Materials Science of Concrete: Sulfate Attack Mechanisms Pp. 73–98. The American Ceramic Society.

Carman, P. C., 1939. Permeability of saturated sands, soils and clays. Journal of Agricultural Science, 29(2), Pp. 262–273. https://doi.org/10.1017/S0021859600020670

Concrete Institute of Australia, Durability Committee. 2015. Recommended practice. Concrete durability series Z7/07 – Performance tests to assess concrete durability. Concrete Institute of Australia.

Damidot, D., Glasser, F. P., 1993. Thermodynamic investigation of the CaO–Al_2O_3–$CaSO_4$–H_2O system at 25°C and the influence of Na_2O. Cement and Concrete Research, 23(1), 221–238. https://doi.org/10.1016/0008-8846(93)90007-F

Das, S., Saha, P., 2018. A review of some advanced sensors used for health diagnosis of civil engineering structures. Measurement, 129, 68–90. https://doi.org/10.1016/j.measurement.2018.07.008

Dhandapani, Y., Santhanam, M., 2020. Investigation on the microstructure-related characteristics to elucidate performance of composite cement with limestone–calcined clay combination. Cement and Concrete Research, 129, 105959. https://doi.org/10.1016/ j.cemconres. 2019. 105959

Fan, L., Bao, Y., 2021. Review of fiber optic sensors for corrosion monitoring in reinforced concrete. Cement and Concrete Composites, 120, 104029. https://doi.org/10.1016/j.cemconcomp.2021.104029

Farny, J. A., Kosmatka, S. H. 1997. Concrete diagnosis and control of alkali-aggregate reactions in concrete. In Concrete Technology Pp. 1–23. Portland Cement Association.

Franus, W., Panek, R., and Wdowin, W., 2015. SEM Investigation of Microstructures in Hydration Products of Portland Cement," in 2nd International Multidisciplinary Microscopy and Microanalysis Congress, E. K. Polychroniadis, A. Y. Oral, and M. Ozer, Eds., Cham: Springer International Publishing, Pp. 105–112.

Gowripalan, N., Cabrera, J. G., Cusens, A. R., Wainwright, P. J., 1990. Effect of curing on durability. Concrete International, 12(2), Pp. 47–54.

Hillel, D., 2012. Soil and water: Physical principles and processes. Elsevier.

Hu, J., 2004. Porosity of concrete: Morphological study of model concrete (Doctoral dissertation). [University/Institution if known].

Hughes, D. C., Amtsbüchler, R., 1986. Pore structure and permeability of hardened cement paste. Magazine of Concrete Research, 38(137), Pp. 230–231. https://doi.org/10.1680/macr.1986.38.137.230

Ideker, J. H., Scrivener, K. L., Fryda, H., Touzo, B., 2019. Calcium aluminate cements. In Lea's Chemistry of Cement and Concrete, Pp. 537–584. Elsevier.

Juenger, M. C. G., Jennings, H. M., 2001. The use of nitrogen adsorption to assess the microstructure of cement paste. Cement and Concrete Research, 31(6), Pp 883–892. https://doi.org/10.1016/S0008-8846(01) 00500-8

Katz, A. J., Thompson, A. H., 1986. Quantitative prediction of permeability in porous rock. Physical Review B, 34(11), 8179. https://doi.org/10.1103/PhysRevB.34.8179

Knudsen, T., 1985. On the possibility of following the hydration of flyash microsilica and fine aggregates by means of chemical shrinkage. Cement and Concrete Research, 15(4), 720–722. https://doi.org/10.1016/0008-8846(85)90043-8

Kosmatka, S.H., Wilson, M. L., 2011. Design and control of concrete mixtures: The guide to applications, methods, and materials. Portland Cement Association.

Krivenko, P., Drochytka, R., Gelevera, A., Kavalerova, E., 2014. Mechanism of preventing the alkali–aggregate reaction in alkali activated cement concretes. Cement and Concrete Composites, 45, 157–165. https://doi.org/10.1016/j.cemconcomp.2013.12.007

Kumar, S., Rai, B., Biswas, R., Samui, P., Kim, D., 2020. Prediction of rapid chloride permeability of self-compacting concrete using multivariate adaptive regression spline and minimax probability machine regression. Journal of Building Engineering, 32, 101490. https://doi.org/10.1016/j.jobe.2020.101490

Leemann, A., Lörtscher, L., Bernard, L., Le Saout, G., Lothenbach, B., Espinosa-Marzal, R. M., 2014. Mitigation of ASR by the use of $LiNO_3$—Characterization of the reaction products. Cement and Concrete Research, 59, 73–86. https://doi.org/10.1016/ j.cemconres. 2014.01. 006

Li, S., Roy, D. M., 1986. Investigation of relations between porosity, pore structure, and Cl^- diffusion of fly ash and blended cement pastes. Cement and Concrete Research, 16(5), Pp. 749–759. https://doi.org/10.1016/0008-8846(86)90065-6

Lichtner, P.C., Steefel, C. I., Oelkers, E.H., 2018. Reactive transport in porous media (Vol. 34). Walter de Gruyter GmbH & Co KG.

Liu, K.-W., Mukhopadhyay, A. K., 2014. A kinetic-based ASR aggregate classification system. Construction and Building Materials, 68, 525–534. https://doi.org/10.1016/j.conbuildmat.2014.06.049

Ma, Y., Guo, Z., Wang, L., and Zhang, J., 2017. Experimental investigation of corrosion effect on bond behavior between reinforcing bar and concrete. Constr. Build. Mater., 152, Pp. 240–249. doi: 10.1016/j.conbuildmat.2017.06.169.

Malhotra, V.M., and Mehta, P.K., 2002. High-performance, high-volume fly ash concrete: materials, mixture proportioning, properties, construction practice, and case histories. Supplementary Cementing Materials for Sustainable Development, Incorporated.

Mamun, K. A., Islam, T., Rahman, M. M., Hossain, M. S., Smart, R., 2019. A prototype of an electromagnetic induction sensor for non-destructive estimation of the presence of corrosive chemicals ensuing concrete corrosion. Sensors, 19(9), 1959. https://doi.org/10.3390/s19091959

McCarthy, M. J., Jones, M. R., Zheng, L., Robl, T. L., Groppo, J. G., 2013. Characterising long-term wet-stored fly ash following carbon and

particle size separation. Fuel, 111, 430–441. https://doi.org/10.1016/j.fuel.2013.02.048

McCarthy, M.J., and Dyer, T.D., 2019. Pozzolanas and pozzolanic materials, 5th ed. Elsevier Ltd. doi: 10.1016/B978-0-08-100773-0.00009-5.

McMillan, F. R., Lyse, I. 1929. Some permeability studies of concrete. Journal Proceedings, Pp. 101–142.

Mehta, P. K. 1980. Pore size distribution and permeability of hardened cement pastes. In Proceedings of the 7th International Congress on Cement Chemistry Pp. VII–1–VII–8.

Mikhail, R. S., Copeland, L. E., Brunauer, S. 1964. Pore structures and surface areas of hardened Portland cement pastes by nitrogen adsorption. Canadian Journal of Chemistry, 42(2), Pp. 426–438. https://doi.org/10.1139/v64-068

Monteiro, P. J. M., Kurtis, K. E. 2003. Time to failure for concrete exposed to severe sulfate attack. Cement and Concrete Research, 33(7), 987–993. https://doi.org/10.1016/S0008-8846(02)01097-9

Monteiro, P. J. M., Kurtis, K. E. 2003. Time to failure for concrete exposed to severe sulfate attack. Cement and Concrete Research, 33(7), 987–993. https://doi.org/10.1016/S0008-8846(02)01097-9

Nandhini, K., and Ponmalar, V., 2021. Effect of Blending Micro and Nano Silica on the Mechanical and Durability Properties of Self-Compacting Concrete. Silicon, 13 (3), pp. 687–695. doi: 10.1007/s12633-020-00475-5.

Natkunarajah, K., Masilamani, K., Amarasinghe, D. A. S., Attygalle, D. 2023. Encapsulated admixtures with temporary coatings for delayed delivery of core material—Review. ACI Materials Journal, 120(1).

Natkunarajah, K., Masilamani, K., Maheswaran, S., Lothenbach, B., Amarasinghe, D. A. S., Attygalle, D., 2022. Analysis of the trend of pH changes of concrete pore solution during the hydration by various analytical methods. Cement and Concrete Research, 156, 106780. https://doi.org/10.1016/j.cemconres.2022.106780

Neville, A. M., Brooks, J. J., 1987. Concrete technology. Longman Scientific and Technical.

Pakravan, H. R., Latifi, M., Jamshidi, M. 2017. Hybrid short fiber reinforcement system in concrete: A review. Construction and Building Materials, 142, 280–294. https://doi.org/10.1016/j.conbuildmat.2017.03.059

Powers, T. C. 1945. Studies of water vapour adsorption of hardened Portland cement paste. Research Laboratories of the Portland Cement Association, Bulletin, 22.

Powers, T. C., Copeland, L. E., Mann, H. M. 1959. Capillary continuity or discontinuity in cement pastes. Journal of the Portland Cement Association Research and Development Laboratories, 1(2), 38–48.

Profile, S. E. E. 2001. Sulphate attack. Structural Survey, 19(2). https://doi.org/10.1108/ss.2001.11019bab.003

Quinn, W., Kelly, G., Barrett, J. 2012. Development of an embedded wireless sensing system for the monitoring of concrete. Structural Health Monitoring, 11(4), 381–392. https://doi.org/10.1177/ 1475921712439992

Ranachowski, Z., Jóźwiak-Niedźwiedzka, D., Ranachowski, P., Dąbrowski, M., Kudela, S., Dvorak, T., 2015. Analysis of pore distribution and connectivity in concrete using X-ray microtomography. In Brittle Matrix Composites 11 - Proceedings of the 11th International Symposium on Brittle Matrix Composites BMC 2015 (pp. 203–212).

Rootare, H. M., Prenzlow, C. F., 1967. Surface areas from mercury porosimeter measurements. Journal of Physical Chemistry, 71(8), 2733–2736. https://doi.org/10.1021/j100871a024

Roy, D. M., 1988. Relationships between permeability, porosity, diffusion, and microstructure of cement pastes, mortar, and concrete at different temperatures. MRS Proceedings, 137, Pp. 179–189. https://doi.org/10.1557/PROC-137-179

Sanchez, L. F. M., Fournier, B., Jolin, M., Bastien, J., 2014. Evaluation of the stiffness damage test (SDT) as a tool for assessing damage in concrete due to ASR: Test loading and output responses for concretes incorporating fine or coarse reactive aggregates. Cement and Concrete Research, 56, Pp. 213–229. https://doi.org/10.1016/ j.cemconres.2013.11.013

Shamsipur, M., Barati, A., Nematifar, Z., 2019. Fluorescent pH nanosensors: Design strategies and applications. Journal of Photochemistry and Photobiology C: Photochemistry Reviews, 39, Pp. 76–141. https://doi.org/ 10.1016/j.jphotochemrev.2019.03.001

Shetty, M. S. 2000. Concrete technology theory and practice: Types of cement (Vol. 055, pp. 1–647). [Online]. Available: https://www.amieindia.in/downloads/ebooks/concrete-tech.pdf

Shi, Z., and Lothenbach, B., 2019. The role of calcium on the formation of alkali-silica reaction products. Cem. Concr. Res., 126, no. September, p. 105898. doi: 10.1016/j.cemconres.2019.105898.

Štukovnik, P., Prinčič, T., Pejovnik, R. S., Bosiljkov, V. B., 2014. Alkali-carbonate reaction in concrete and its implications for a high rate of long-term compressive strength increase. Construction and Building Materials, 50, Pp. 699–709. https://doi.org/10.1016/ j.conbuildmat.2013.10.017

Stutzman, P., Leigh, S., 2010. Statistical calibration of ASTM C150 Bogue-derived phase limits to directly determined phases by quantitative X-ray powder diffraction. Journal of ASTM International, 7(7), 1–8. https://doi.org/10.1520/JAI102273

Tafraoui, A., Escadeillas, G., and Vidal, T., 2016. Durability of the Ultra High Performances Concrete containing metakaolin. Constr. Build. Mater., 112, Pp. 980–987. doi: 10.1016/j.conbuildmat.2016.02.169.

Tang, S. W., Yao, Y., Andrade, C., Li, Z. J., 2015. Recent durability studies on concrete structure. Cement and Concrete Research, 78, 143–154. https://doi.org/10.1016/j.cemconres.2015.06.018

Tumidajski, P. J., Lin, B., 1998. On the validity of the Katz-Thompson equation for permeabilities in concrete. Cement and Concrete Research, 28(5), Pp. 643–647. https://doi.org/10.1016/S0008-8846(98)00037-4

Tutti, K., 1982. Corrosion of steel in concrete (Ph.D. thesis). Lund University, Swedish Cement and Concrete Research Institute.

Uysal, M., Akyuncu, V., Tanyildizi, H., Sumer, M., Yildirim, H., 2019. Optimization of durability properties of concrete containing fly ash using Taguchi's approach and ANOVA analysis. Revista de la Construcción, 17(3), 364–382. https://doi.org/10.7764/ RDLC.17.3.364

Van Breugel, K. 1993. Simulation of hydration and formation of structure in hardening cement-based materials (Doctoral dissertation). Delft University of Technology.

Wang, X.F., Zhang, J.H., Zhao, W., Han, R., Han, N.X., and Xing, F., 2018. Permeability and pore structure of microcapsule-based self-healing cementitious composite. Constr. Build. Mater., 165, Pp. 149–162. doi: 10.1016/j.conbuildmat.2017.12.008.

Yamada, K., et al., 2014. CPT as an evaluation method of concrete mixture for ASR expansion. Construction and Building Materials, 64, 184–191. https://doi.org/10.1016/j.conbuildmat.2014.04.023

Ye, G., 2005. Percolation of capillary pores in hardening cement pastes. Cem. Concr. Res., 35 (1), pp. 167–176. doi: 10.1016/j.cemconres.2004.07.033.

Ye, G., and Van Breugel, K., 2009. Simulation of connectivity of capillary porosity in hardening cement-based systems made of blended materials. Heron, 54 (2–3), pp. 161–182.

Zhang, Y. 2008. Mechanics of chloride ions transportation in concrete (Doctoral dissertation). Zhejiang University, Hangzhou, China.

Zhang, Y., Ye, G. 2019. A model for predicting the relative chloride diffusion coefficient in unsaturated cementitious materials. Cement and Concrete Research, 115, 133–144. https://doi.org/10.1016/j.cemconres.2018.10.013

Zhang, Y., Yang, Z., Ye, G. 2020. Dependence of unsaturated chloride diffusion on the pore structure in cementitious materials. Cement and Concrete Research, 127, 105919. https://doi.org/10.1016/j. cemconres.2019.105919

Zhou, T., Ioannidou, K., Ulm, F. J., Bažant, M. Z., Pellenq, R. J. M. 2019. Multiscale poromechanics of wet cement paste. Proceedings of the National Academy of Sciences of the United States of America, 116(22), 10652–10657. https://doi.org/10.1073/pnas.1901160116

Zongjin, L., 2011. Advanced concrete technology. Hoboken, NJ: John Wiley and Sons, Inc.

Zuo, J., Zhan, J., Dong, B., Luo, C., Liu, Q., & Chen, D. (2017). Preparation of metal hydroxide microcapsules and the effect on pH value of concrete. Construction and Building Materials, 155, 323–331. https://doi.org/10.1016/j.conbuildmat.2017.07.155